Mobility and Stability Evaluation in Wireless Multi-Hop Networks Using Multi-Player Games

F. Fitzek L. Badia M. Zorzi
DipInge, Università di Ferrara
via Saragat 1, 44100 Ferrara
Italy
frank@fitzek.net
lbadia@ing.unife.it
zorzi@ing.unife.it

G. Schulte P. Seeling
acticom GmbH
mobile networks
Am Borsigturm 42
13507 Berlin
Germany
schulte@acticom.de
seeling@acticom.de

T. Henderson
Dept. of Computer Science
University College London
Gower Street
London WC1E 6BT
United Kingdom
T.Henderson@cs.ucl.ac.uk

ABSTRACT

Plenty of work was contributed in the field of protocol design and performance evaluation of multi-hop networks. It is generally accepted that mobility has a huge impact on the protocol performance; even more for multi-hop networks. Obtaining realistic measurements of mobility, however, is complex and expensive. Thus, we adopt virtual world scenarios to explore the mobility issue, by using the well-known multi-player game, Quake II. The advantage of the Quake II engine is that users move within virtual worlds under realistic constraints, whereas other mobility models may offer insufficient accuracy or operate under unrealistic assumptions. Moreover, it is very easy to create new virtual worlds and to adapt them to specialized needs. In this paper, we propose an analytical framework for mobility measurements in virtual worlds that could be adopted for the design of communication protocols. Our framework enables the study of the impact of mobility on connectivity and stability of the network, giving useful insights for improving communication performance. An interesting application of our approach is the analysis of coverage extension of so called hotspots or emergency situations, where the fixed network infrastructure is insufficient or non-existent. In these extreme cases, multi-hop networks can be used to set up communication quickly. As these situations comprise a plethora of different cases and scenarios, our model is appropriate for their analysis, due to its generality. We use our framework to investigate the performance of multi-hop networks based on IEEE 802.11a technology. In contrast to other contributions focusing only on connectivity, the IEEE 802.11a technology also considers multi-rate connections. Our framework covers the evaluation of simple connectivity as well as link quality stability in the presence of mobility, a combination that has not been considered thus far. Therefore we introduce two simple routing schemes and highlight the performance of these protocols in the presence of mobility. Furthermore we come up with four definitions of stability and investigate protocols for multi-hop networks in terms of this parameter. Our other contributions are the changes to the Quake II engine and the availability of mobility trace files.

NETGAMES '03 Redwood City, CA, USA

Keywords

ad hoc networks, multi-hop networks, IEEE 802.11a, capacity, mobility, stability, connectivity, routing, Quake II, multi-player, trace data

1. INTRODUCTION

Multi-hop networks have gained a lot of interest in recent years. Initial applications targeted the military sector, but one current use of these networks is to extend the coverage of wireless networks. Using multi-hop capability to extend coverage can dramatically reduce the installation costs of wireless networks. The performance of multi-hop networks, however, depends on the routing mechanism used, and much research has been carried out in this field. The routing itself is dependent on the nodes' mobility and the link quality. User mobility can have a huge impact on the performance on communication protocols, but mobility measurements in the real world are highly complex and costly. Therefore, assumptions about mobility will influence the performance of the routing and affect the entire communication system. Existing mobility models are based on random processes. These models, however, fail to consider geometric boundaries (see Section 2). It is unclear whether such models are applicable to real world situations, since different usage scenarios such as public hotspots, military, police, or firefighters, may differ in their communication patterns, due to different geometric boundaries, type of mobility, and so on.

The aim of this paper is to introduce a framework for mobility measurements in virtual worlds, which in turn can be used for the design of new communication protocols. The virtual world that we use is based on the popular multiplayer game *Quake II*. To demonstrate the framework, we use mobility measurements from *Quake II* sessions to investigate the impact of mobility on the performance of multi-hop networks based on IEEE 802.11a technology in conjunction with possible routing schemes. By means of the IEEE 802.11a technology we will show the applicability of our approach to investigation in real networks.

The paper is organized as follows: in Section 2 we give a short overview of related work, where we address the shortcomings of existing mobility models and advocate the use of our approach. Multi-hop networks based on IEEE 802.11a technology are introduced in Section 3. In Section 4 we present our approach and introduce the elements of our testbed and present the calculation of connectivity, mean hop, and mean bandwidth for multi-hop networks. The main results of our mobility and stability evaluation are presented in Section 5. We conclude our work in Section 6 and give a brief outlook for further studies in Section 7.

2. RELATED WORK

Simulations to test the impact of mobility in ad hoc networks are generally performed in very simplistic scenarios. The two most popular models are the *Random Walk* and *Random Waypoint* models. A good overview of these models, as well as others including *Random Direction*, *Gauss-Markov* and *Probabilistic Random Walk*, is provided in [1].

The Random Walk and Random Waypoint models are both based on the concept of Brownian motion. The difference between the two models is the inclusion of pause times. A general problem of these approaches is the overall formulation of human movement into complete random motion. As outlined in [1], nodes are modeled to return to their point of origin with probability $P(X(n) = X(0)) = 1.0$ as n increases to inf. In simulations, this reduces the traveling distances of the nodes. In addition, nodes move randomly, without considering the likelihood of directional changes in human movement direction (e.g., consider the amount of 180 degree turns in normal daily life) and speed (e.g., the state changes between running and standing still). When the model is enhanced with the addition of pause (i.e., standing still) times, it becomes more realistic. However, due to the stateless behavior, the enhanced model is still unable to map human movement behavior correctly. A good explanation of the shortcomings of the latter model is given in [2] for the example of network protocol modeling with respect to the mean node movement.

The Probabilistic Random Walk model enhances the Random Walk model by regarding the states of speed and direction for a given node. This model is introduced by Chiang in [3]; it uses a transition matrix that takes the node's current movement into account and determines the next position of a node in terms of Cartesian coordinates. This model is able to capture human motion on various levels. Firstly, the transition matrix definition allows one to set the higher probabilities of following a certain direction of movement, as it is in real world scenarios (i.e., in the case that we are not considering obstacles). Secondly, the model is able to capture pauses in the node's (or human's) movement with probabilities of no change in the set of (X, Y) coordinates.

From the point of view of the environment, however, all of these models assume that movement in any direction, and of any kind, is possible on an infinite plane. The effects of objects or other users are only considered to be ethereal. Other researchers, however, have taken more realistic mobility models into account, in an attempt to avoid behaviors that do not occur in the real world. Elmallah *et al.* [4] consider a trade-off between deterministic paths and a random choice of these paths. Each terminal has a set of possible positions, connected with fixed routes. Positions change according to a semi-Markov process, i.e., each user spends a random time in a given position, before randomly choosing its next position. A similar approach is considered by Tian *et al.* [5], who present a graph-based mobility model. In this case, the points move on the edge of differently-connected graphs. This can be useful, for instance, for considering pedestrian mobility in cities with a very constrained infrastructure. Johansson *et al.* introduce obstacles in [6], but the effects of these are mainly limited to propagation. The users are not permitted to go straight through obstacles, but this only manifests itself by considering links that cross obstacles to be broken.

In all of these studies, mobility models are mainly used to study the performance of routing protocols, using common metrics such as end-to-end delay. Wang and Li analyze the performance of well-known group mobility models using novel metrics in [7]. In particular, the Reference Point Group Mobility Model is extended to a wider model and the partitioning of the network is used as a metric for evaluation.

Instead of using a model for mobility, we propose to use a virtual world for simulation, since this allows all of the above effects to be taken into account. This approach presents many advantages. Obstacles and infrastructure can be considered, not only in preventing the connectivity, but also for the mobile users' choice of path. For instance, rivers or highways in the real world (or the lava pools in our *Quake II* scenario) can often be impossible or difficult to cross, even though they do not block network propagation. Moreover, in a virtual world scenario, it is impossible for different users to occupy exactly the same position simultaneously, as in the real world. The effects of moving to avoid other people can also be considered. Motion in a virtual world is more realistic than one-dimensional movement on a graph-edge, and includes the possibility for three-dimensional movement. Finally, although we do not consider this in this paper, the impact of group mobility can be considered, for example by using scenarios within a team-based game.

3. MULTI-HOP NETWORKS

Multi-hop networks are gaining a lot of interest lately. Actual implementations of multi-hop networks are based on IEEE 802.11b. This IEEE standard is the leading Wireless Local Area Network (WLAN) technology in the world, and researchers around the world are working on improvements to the standard. The new IEEE 802.11a standard [8] differs from IEEE 802.11b in the design of the physical layer. By utilizing the 5 GHz ISM band, up to 12 channels can be used in parallel (at least in the US, since this is dependent on government regulations). Link adaptation is also used, which leads to seven possible data rates for communication. A link-level simulator was developed using MATLAB [9] at the University of Ferrara, to investigate the performance of IEEE 802.11a enabled wireless nodes in a two-dimensional space. The wireless link model takes path loss, correlated shadowing, and Jakes' multi-path fading into consideration. Figure 1 gives the data rate between two IEEE 802.11a wireless nodes as a function of their distance. Figure 1 was generated by considering a network consisting of two nodes in the simulator. Specifically, a node was randomly positioned within a $300 \times 300\text{m}^2$ area. A second node was then positioned at distance d from the first node. The distance d was increased by 10 cm for each measurement, and for each position a number of samples were considered. The procedure was repeated over one million times. The simulation parameters are summarized in Table 1. We note that Bing [10] presents a similar relationship between data rate and range

by means of indoor measurements with IEEE 802.11a equipment. In a multi-hop network multiple nodes communicate with each other. The data rate depends on the link quality, which may change in case nodes are moving around.

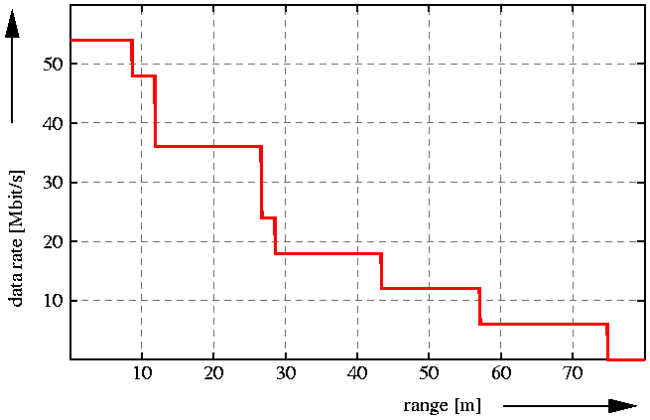

Figure 1: Data rate versus range.

The impact of mobility is shown by means of two different routing schemes. Due to the multi-rate connection between nodes, different routes can be chosen. One possibility would be to take the *shortest path*, that is, the route with the lowest number of hops. A second possibility would be to choose the route with the *largest bandwidth* of each hop. The latter may lead to a higher number of hops, but may also lead to a higher level of bandwidth. In the case of a multi-hop connection, we take the minimum bandwidth of all the individual links as the bandwidth of the overall connection. The connection with the smallest bandwidth value is referred to as the *bottleneck*. As an example we refer to Figure 2. A source node may convey data to the destination node by using either the *shortest path* approach or the *largest bandwidth* approach. In the former case the source node sends directly to the destination with a data rate of 6 Mbit/s. In the latter case links with the highest bandwidth are used to convey data towards the destination. Even if the first two hops offer 54 Mbit/s, the overall data rate depends on the link with the lowest data rate; in this case 18 Mbit/s, which is caused by the third link representing the bottleneck. In general, the largest bandwidth approach leads to higher bandwidth values with an increased number of hops.

We use the parameter settings given in Table 1 to show the impact of our mobility model on an IEEE 802.11a based multi-hop network. In Figure 3 a possible distribution of nodes and their related data rates is given. The concentric circles around a player identify the different data rate zones. Darker colors represent higher data rates. The network is fully connected. Clustering at high data rates is given if a group of players is located nearly at the same place. This plot was generated with the ViTAN tool [11] and the IEEE 802.11a extensions.

4. OUR APPROACH

To create a more realistic mobility model than the random processes described in Section 2, we decided to use multi-player games, and measure the mobility of the players in the game's virtual world. The software for multi-player games such as *Quake* and *Half-Life* is no longer limited to games, but it is also used to emulate the real world. One of the first examples of this crossover was researchers at Cambridge University, who were investigating electronic communication between buildings' architects and their eventual users [12, 13, 14]. The computer game *Quake II* was modified to allow the architects' clients to move within virtual buildings. The source code to *Quake* and *Quake II* has been made freely available, and so it is possible to replace the scenery, avatars, and to remove items such as weapons. The door is therefore wide open to create new applications.

4.1 The testbed

The testbed was used for the mobility measurements. After the traces were collected, we used a post-processor to investigate the impact on the protocol performance. This approach is valid as long as we do not assume any feedback from the communication quality back to the game. We come back to this discussion in Section 7. In the following subsections we describe our testbed.

4.1.1 The server

Quake II is a First Person Shooter (FPS) game, introduced by id Software in 1996. At the time, it was one of the most popular games of its type, and it is the most recent FPS game for which the source code is available.

We used version 0.15 of the fork of the original *Quake II* code that can be found at `http://icculus.org/quake2/`. This code differs from the original id Software release in that it is easier to compile under Linux, and includes a few enhancements. The server was modified to log the positions of each player in the virtual world. The positions were logged every time the server updated a frame. Our modified server can be found at [15].

A modified *Quake II* server was set up at UCL in London. The server comprised a 1.2GHz Athlon running Linux kernel version 2.4.9, and was advertised via the standard *Quake II* master server mechanisms (see [16] for details). In spite of the game's age, we observed players connecting to the server within days of the server being initially advertised.

Listing 1 shows an example trace file. The first column shows the server's internal clock time in milliseconds. The next column indicates a player's IP address and port number. The three values in brackets give the player's position in Cartesian coordinates. The last column shows the application-level delay, or "ping" time, of each player. In this given example three players are connected to the server. At each frame update, approximately every 100 ms, the players' positions are written to the trace file.

4.1.2 The clients

As the server was modified to log all of the players' positions, no changes were necessary at the client. This approach allows a large number of players world-wide to participate in our measurements, as previous experiments have indicated that players may be unwilling to download untrusted or additional client code. In our experiments we used the Windows *Quake II* client, version 3.20.

4.1.3 The map

For our measurements we created our own virtual world by generating a new level, or map, for the game. The map consisted of a plain box, with no additional objects inside it. Figure 4 shows a screen-shot from the editor used to create the map: the top left shows a plan view of the map with the "spawn points" highlighted. These spawn points

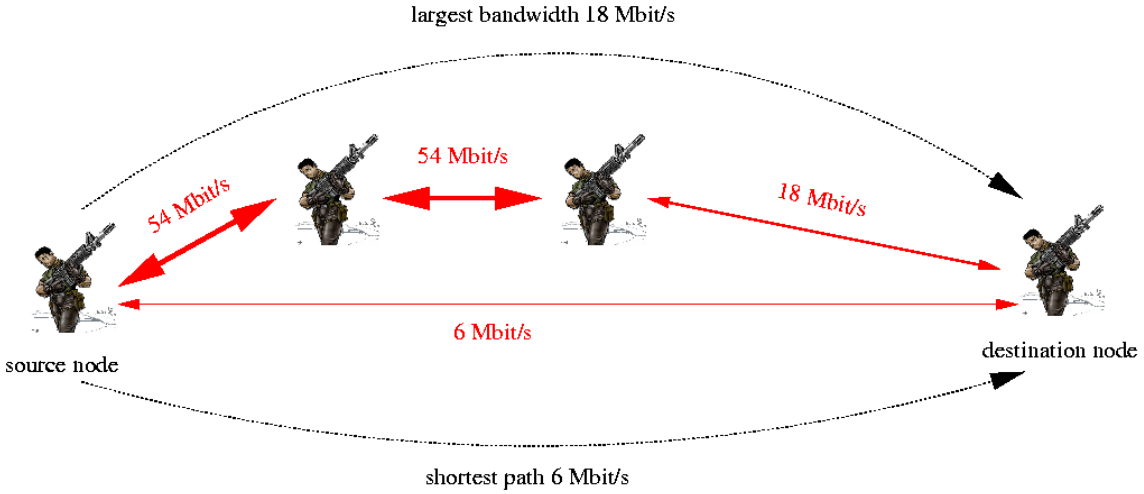

Figure 2: Example of two different routing schemes.

Table 1: Parameters for the IEEE 802.11a simulator.

parameter	value	info
receiver sensitivity	-70	in dBm
alpha	3.5	distance attenuation coefficient
sigma	6	standard deviation for the lognormal fading in dB
attconst	-21	attenuation at 1 meter of distance in dB

are the locations at which players can enter the map; these were randomly placed at the edge and center of the map. The map was designed to be as large as the *Quake II* engine would allow - approximately 4000 by 4000 units in the measurements of the map editor. We scaled the length unit in such a way that we have a 150m by 150m box. The map only consisted of one floor, and was therefore two-dimensional in that players could not move along the z-axis (apart from jumping up and down).

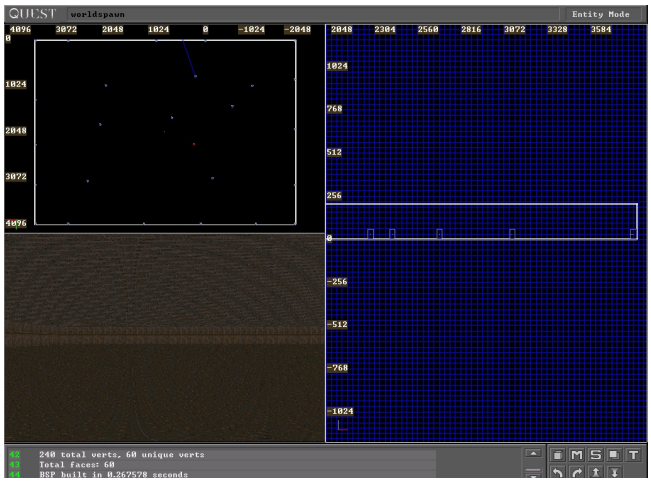

Figure 4: Map editor showing the map used for our measurements.

4.1.4 The players

Thirteen student volunteers played the game at the University of Ferrara. For the purposes of our measurements the players were asked not to shoot at each other, but instead to move around and explore the virtual world.

4.2 Analysis of the trace data

For the analysis of the trace data we present the following general approach. We assume J virtual players, where each player's position is characterized by a vector $P_j(t)$

$$P_j(t) = \begin{pmatrix} x_j \\ y_j \\ z_j \end{pmatrix} \tag{1}$$

of Cartesian coordinates x, y, and z. The coordinates may change with the player's mobility in every time slot t. For further calculation we need the distances between the players in the virtual world to derive the related data rate for the IEEE 802.11a multi-hop communication (see Section 3). The distance matrix $\overline{D}$ is given by

$$\overline{D}(t) = \begin{pmatrix} d_{1,1} & \dots & d_{1,J} \\ \dots & d_{i,j} & \dots \\ d_{J,1} & \dots & d_{J,J} \end{pmatrix}, \tag{2}$$

where $d_{i,j}$ represents the distance between node i and j. The distance is given by

$$d_{i,j} = \sqrt{(x_i - x_j)^2 + (y_i - y_j)^2 + (z_i - z_j)^2}. \tag{3}$$

From this we can derive the single hop connectivity matrix $\overline{A}(t)$ (given in Equation 5). As given in Equation 4, the matrix A consists of the two symbols `0` and `1`. In the case where $a_{i,j}$ is `0`, there is no direct connection between wireless node i and j. Otherwise $a_{i,j}$ is set to `1`. The existence of a direct connection between i and j can be gathered from Figure 1, where the data range of an IEEE 802.11a communication scheme is given in terms of the distance between sender and receiver. The maximum distance at which the minimum data rate of 6 Mbit/s can be achieved is $D_{MAX} = 75m$.

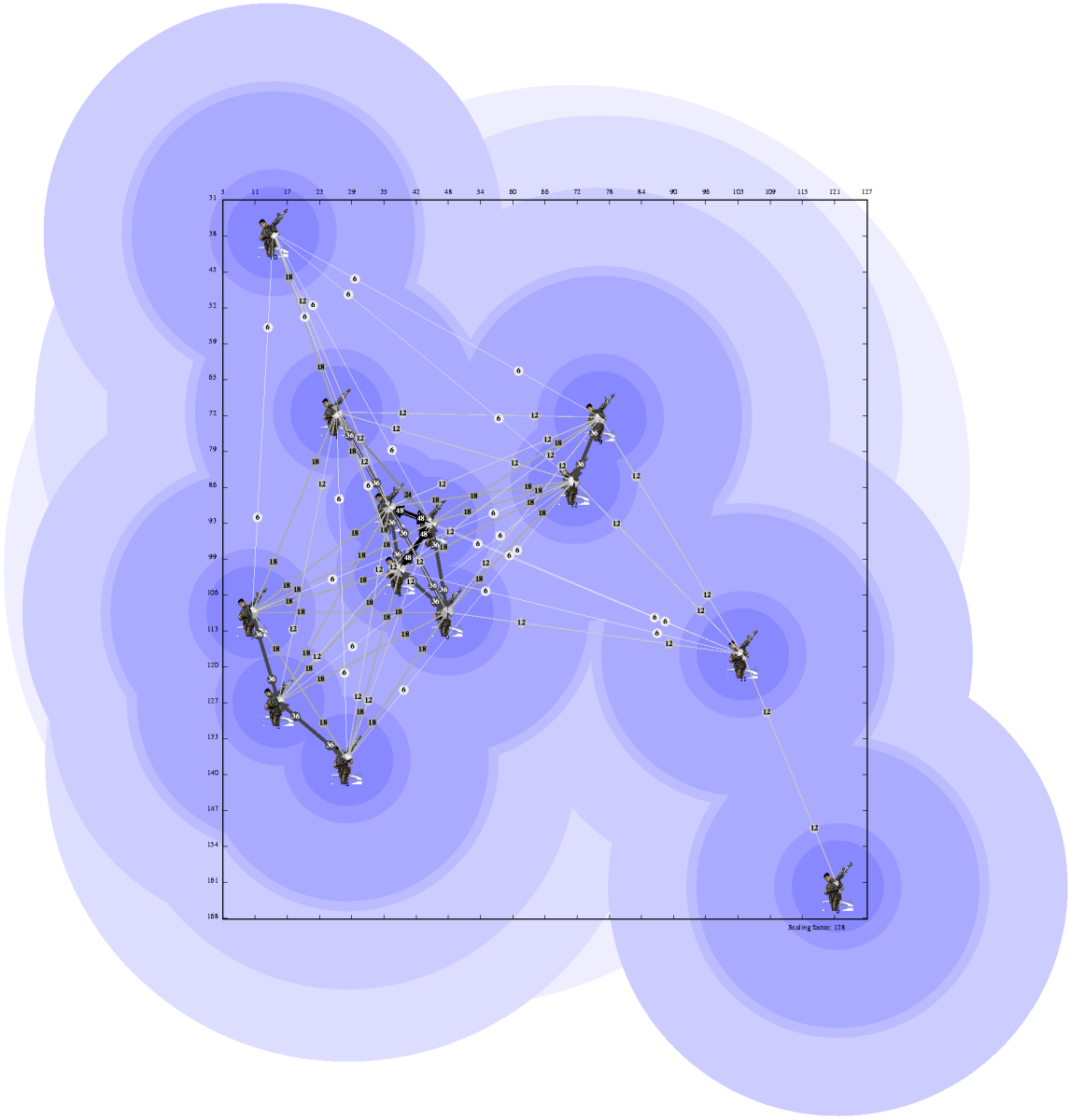

Figure 3: Example of an IEEE 802.11a based Multi-hop Network.

$$a_{i,j} = \begin{cases} 0 & : \quad d_{i,j} > D_{MAX} \\ 1 & : \quad d_{i,j} < D_{MAX} \end{cases} \tag{4}$$

$$\overline{A}(t) = \begin{pmatrix} a_{1,1} & \dots & a_{1,J} \\ \dots & a_{i,j} & \dots \\ a_{J,1} & \dots & a_{J,J} \end{pmatrix} \tag{5}$$

For the multi-hop case we have to calculate the multi-hop connectivity matrix $\overline{C}$. The matrix $\overline{C}$ reflects the situation where two wireless terminals can communicate with each other by means of other terminals' multi-hop capability. If $d_{i,j} > D_{MAX}$, direct communication is not possible, and neighboring nodes forward the packets to the target node. The elements $\{c_{i,j}\}$ of matrix $\overline{C}$ represent the number of hops needed to reach the destination node. The values of these elements will change depending on the chosen routing algorithm.

$$\overline{C}(t) = \begin{pmatrix} c_{1,1} & \dots & c_{1,J} \\ \dots & c_{i,j} & \dots \\ c_{J,1} & \dots & c_{J,J} \end{pmatrix}, \tag{6}$$

The procedure to calculate $\overline{C}$ is given in [17, 18, 19]. For a better understanding of our methodology, we present a short description of the algorithms. Suppose that an auxiliary matrix $\overline{B}$ is appropriately defined. Its role will be discussed in the following. The matrix $\overline{C}$ is calculated using the following steps:

1. INITIALIZATION: we define $\overline{C}^1 = \overline{A}^1$, a third intermediate matrix $\overline{B}^1$=0 m=2
2. START: set $\overline{A}^{(m)} = \overline{C}^{(m-1)} \cdot \overline{C}^{(m-1)}$
3. calculate $\overline{B}^{(m)}$

4. if ($\forall$ i,j $b_{i,j} = 0$) STOP
5. recalculate $\overline{C}^{(m)} = \overline{C}^{(m-1)} + \overline{B}^{(m)}$
6. m++
7. GOTO START

The only missing item is how to calculate matrix $\overline{B} = \{b_{i,j}\}$. Details of how to calculate this are given in Equation 13 in the Appendix.

Once we have calculated the multi-hop matrix $\overline{C}$, the multi-hop connectivity is calculated by simply summing all of the existing connections (represented by matrix elements with values larger than zero) and dividing this by the number of possible connections. This approach is similar to those adopted in [20] and [21].

$$\overline{c}(t) = \frac{\sum_{i=1,\forall i \neq j}^{J} c^*_{i,j}}{J(J-1)}, \tag{7}$$

In Equation 7 the calculation of the multi-hop connectivity $\overline{c}(t)$ is given, with $c^*_{i,j} = 1$ if $c_{i,j} \geq 1$ and $c^*_{i,j} = 0$ otherwise. Apart from the connectivity, the other interesting parameter in this equation is the mean number of hops. Each hop introduces an additional delay in conveying the data from the originating host to the final host. Furthermore, energy is consumed by each forwarding process. For the calculation of the mean hop number $\overline{h}(t)$ we sum up the elements of the multi-hop connectivity matrix and divide it by the number of possible connections (full meshed bi-directional network $J(J-1)$).

$$\overline{h}(t) = \frac{\sum_{i=1,\forall i \neq j}^{J} c_{i,j}}{J(J-1)} \tag{8}$$

Using the relationship between distance and data rate, the single hop data rate matrix $\overline{S}$ can be derived. The calculation is similar to that of the multi-hop and is presented in [17]. As given in Equation 14, the matrix S contains the single hop data rate between two nodes.

$$\overline{S}(t) = \begin{pmatrix} s_{1,1} & \dots & s_{1,J} \\ \dots & s_{i,j} & \dots \\ s_{J,1} & \dots & s_{J,J} \end{pmatrix}, \tag{9}$$

The multi-hop data rate matrix $\overline{M}$ is defined as

$$\overline{M}(t) = \begin{pmatrix} m_{1,1} & \dots & m_{1,J} \\ \dots & m_{i,j} & \dots \\ m_{J,1} & \dots & m_{J,J} \end{pmatrix}, \tag{10}$$

and it is calculated similar to the multi-hop connectivity using a modified version of Equation 13 as given in [17].

The mean multi-hop data rate is then calculated by dividing the sum of all bandwidth achieved by all possible connections such that

$$\overline{m}(t) = \frac{\sum_{i=1,\forall i \neq j}^{J} m_{i,j}}{J(J-1)}. \tag{11}$$

For the design of routing protocols it is very important to investigate the stability of the network. Stable networks need less signaling overhead. For single rate systems the choice of the route was easy as long as the bandwidth of each connection was the same. The parameter for optimization was the number of hops. With multi-rate systems such as the IEEE 802.11a system the routing becomes more complicated.

Different metrics can be used to measure the stability of the system. One possible choice is the standard deviation of the mean data rate of the multi-hop network. Using this metric, situations with a stationary or oscillating rate can be distinguished. The frequency of the oscillations, however, is not made apparent. Thus, we add the measure of the occurrence of a simple variation in the achievable data rate. That is, we consider the ratio between the number of samples in which a change is observed versus the number of total time samples. Formally, this indicator of stability ρ_s can be expressed (for each user i) as:

$$\rho_{s,i} = \frac{\text{number of}(\{t : m_{i,j}(t) \neq m_{i,j}(t-1)\})}{\text{total number of samples}}. \tag{12}$$

In many situations, this metric can be interesting, as sudden changes in the perceived data rate can be important events, e.g., for emergency situations. Some applications may need a minimum guaranteed data rate, even for connections established on-the-fly, and the extreme variability of the applicable paths should be hidden. Note that, when the multi-hop rate is considered, the value of ρ_s is affected mainly by the *bottleneck* link. A possible extension of this metric can be a measure that is able not only to distinguish between frequent or rare variations of the connectivity, but is also able to consider the width of the oscillations. To achieve this, a *weighted number of changes* can be considered. In this metric, a rate threshold $r_{i\theta}$ is defined for each user i. This threshold can be seen as a quality constraint, that is, the minimum guaranteed rate for the majority of the applications. When the changes in the rate have the additional drawback of crossing the threshold, they are accounted for with a higher coefficient k, e.g., 12. The definition of the modified stability ratio ρ'_s for the ith user is given in Equation 15. We propose the mean value of ρ_s as a stability metric, called *mean stability ratio* in the following discussion.

Furthermore we introduce another measurement that can be useful to describe the stability of the network, i.e. the evaluation of the time between two different rate changes. This can be studied with a probabilistic approach, i.e., by analyzing the probability density function (PDF) $\psi(t)$ of the time between two rate variations. This PDF can be transformed into a cumulative function, so that an evaluation of the mean achievable time without rate changes. Finally, the *mean stability time* τ_s can be defined as the mean time between two changes, i.e., τ_s is the expected time during which no variation of the rate occurs. This value gives a reasonable expectation of the time for which an application can exploit a constant channel.

5. RESULTS

The trace data of all players in the virtual world were collected at the server. Using this trace data, we were are able to determine the location of each node within our virtual world. As an example we give the location of one player over the time in Figure 5.

From the node's mobility it is easy to derive the speed and

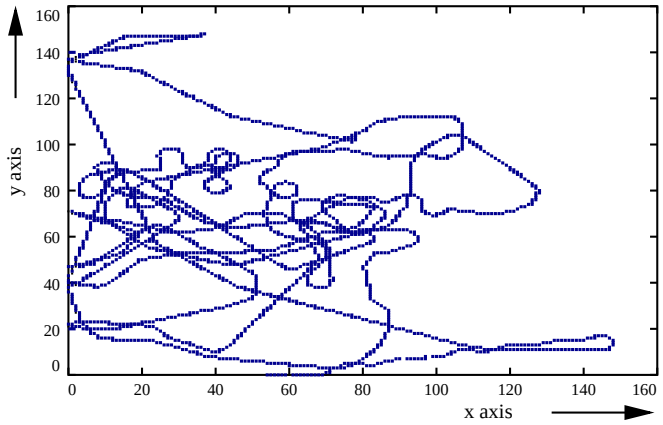

Figure 5: Mobility of one user in the plain box scenario.

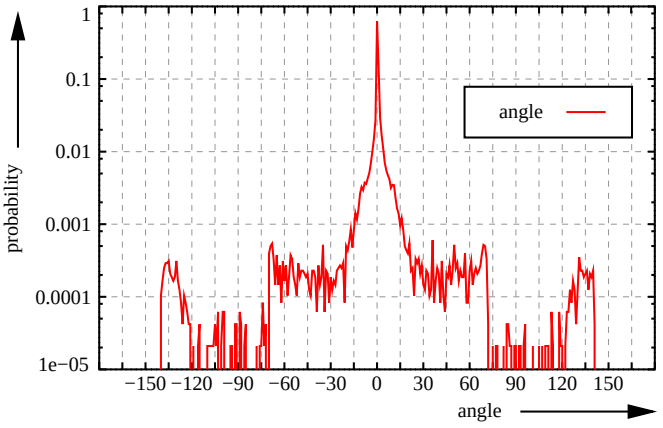

Figure 6: Changes in the moving direction.

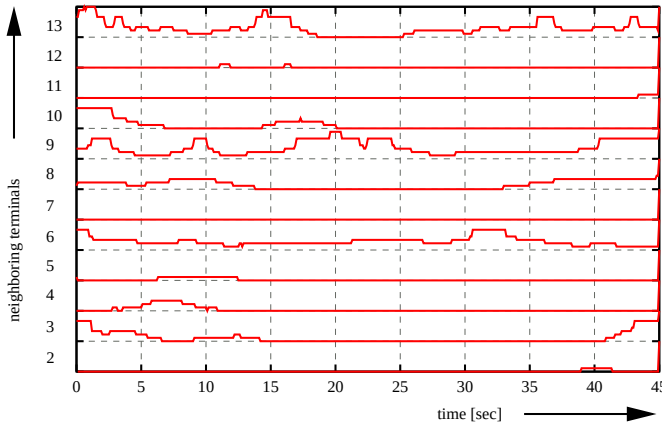

Figure 7: Available bandwidth of a direct communication between node 1 and all other nodes.

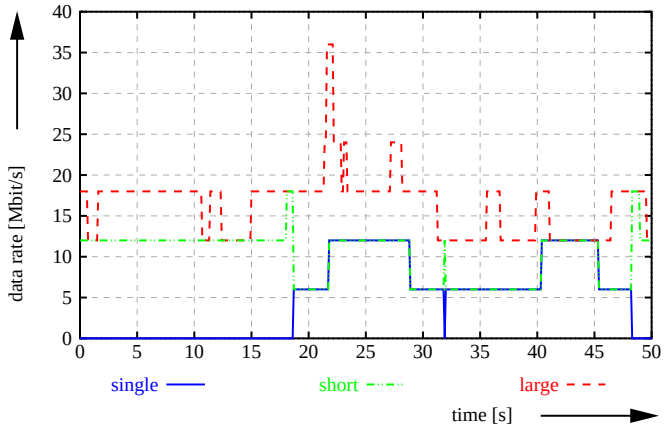

Figure 8: Available bandwidth between node 1 and node 13 using a single hop connection, multi-hop with *shortest path*, and multi-hop with *largest bandwidth*.

the angle of movement. In Figure 6 the change in the moving direction is given. Obviously changes occur more frequently in the virtual player's viewing angle ($-70° \cdots + 70°$) than in the other directions of movement. Note that existing mobility models such as the random waypoint do not include such effects.

As we explained in Section 4.2, we are able to derive the data rate between wireless terminals based on their locations. In Figure 7 the available bandwidth of a direct communication between node 1 and all other nodes is given. From this simple plot, the variance in the existing communication can be shown. Figure 7 gives the single hop data rate between nodes. On the y-axis the different mobiles are listed with their data rate. The data rate of the nodes are shifted on the y-axis for a better illustration.

In Figure 8 the available bandwidth between node 1 and node 13 is given for a time window of 50 seconds using a single hop connection, a multi-hop with *shortest path*, and a multi-hop with *largest bandwidth*. As both nodes are moving nearly all the time, the link adaptation of IEEE 802.11a changes the data rate depending on the distance between these two nodes. The single hop connection offers the lowest available bandwidth. The larger the distance between the nodes, the lower the available data rate. A situation may even arise where no communication is possible at all. Using the *shortest path* multi-hop approach offers higher data rates than single hop. In this case the coverage is extended by the multi-hop capability of the network. This capability is also used for the *largest bandwidth* approach. With this approach even higher data rates can be achieved. The cost of this approach is that a higher number of hops that has to be used.

The multi-hop connectivity $\overline{c}(t)$ as defined in Equation 7 versus time for 13 nodes is given in Figure 9. Most of the time the network is fully connected ($\overline{c}(t) = 1$). But in case of only one disconnected terminal the connectivity level decreases to $11/13 = 0.84$. Thus, the given example reflects the situations in which up to four terminals are not connected to the multi-hop network (e.g. time instant 275 s) in Figure 9.

In Figure 10 the mean number of hops $\overline{h}(t)$ versus time for the two different routing schemes is given. The *shortest path* approach is represented by a solid line, while the *largest bandwidth* approach is represented by a dashed line. It can be seen that the *largest bandwidth* choice leads to a higher number of hops than the *shortest path* approach. While the *shortest path* approach yields values never higher than 2.5, the *largest bandwidth* approach can go up to a value of 4 hops.

For the two routing approaches, the mean multi-hop bandwidth $\overline{m}(t)$ versus time is given in Figure 11. As expected,

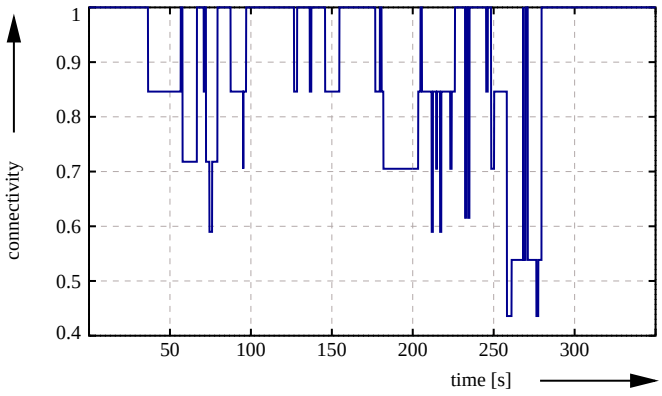

Figure 9: Multi-hop connectivity $\overline{c}(t)$ versus time for 13 nodes.

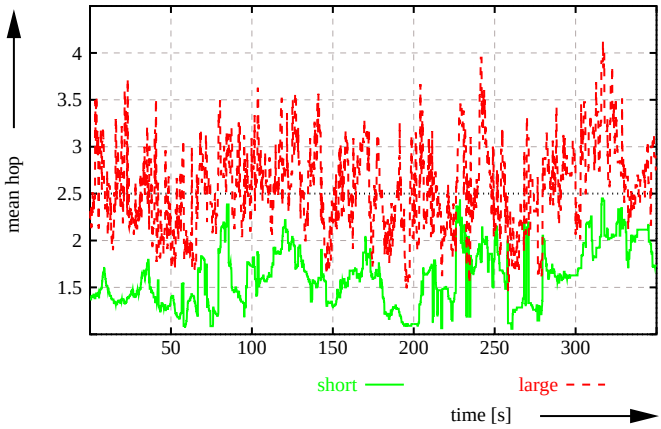

Figure 10: Mean number of hops $\overline{h}(t)$ versus time for two different routing schemes.

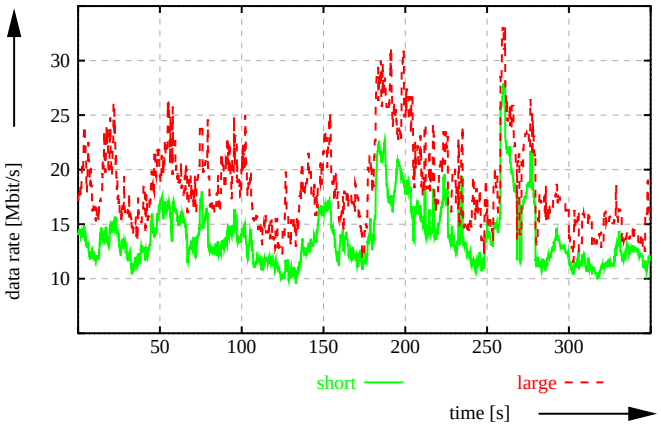

Figure 11: Mean multi-hop bandwidth $\overline{m}(t)$ versus time for two different routing schemes.

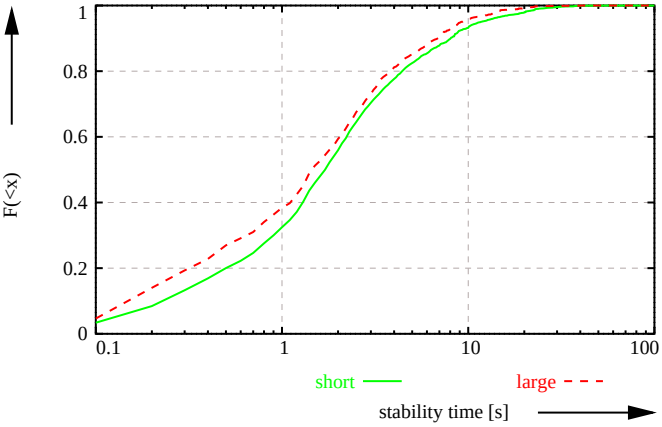

Figure 12: Cumulative stability PDF ψ without any threshold.

the bandwidth values of the *largest bandwidth* approach are larger than those of the *shortest path* approach. The latter approach has bandwidth values between 10 and 27 Mbit/s, while the former approach leads to values between 12 and 34 Mbit/s.

The stability measurements defined in the previous section have been analyzed for the two routing schemes. The first result is the mean stability ratio for the whole network, that is $\rho_s = 0.03008$ and $\rho_s = 0.03695$ for the *shortest path* and the *largest bandwidth*, respectively. This means that a rate variation is observed approximately once every 33 or 27 time slots, respectively. The mean stability time τ_s is $\tau_s = 3.3$ s and $\tau_s = 2.7$ s for the *shortest path* and the *largest bandwidth*, respectively.

In Figure 12 the cumulative stability PDF $\psi(t)$ is represented. It can be seen that a change in rate is almost certain to occur within ten seconds. Thus, applications that require a constant channel support for a longer time may have problems under the examined scenario. The higher stability of the *shortest path* approach can be intuitively justified as follows: as the number of hops is lower, it is less likely that a variation in the bottleneck rate occurs. Furthermore, the *shortest path* approach does not use the full spectrum of data rates. It is unlikely that, e.g., 54 Mbit/s is used for a multi-hop connection. This implies that in emergency situations, where it is probably more important to have a constant service than a relatively high quality, the *shortest path* approach might be more suitable. In any case, note that the stability indicators, as previously defined, are not very high in both cases; thus, adjustments in order to directly improve stability can also be useful.

In case we limited the changes only to situations were the bandwidth is below 12 Mbit/s, the *largest bandwidth* approach is more stable than the *shortest path* approach as given in Figure 13. This is due to the higher bandwidth achieved by the *largest bandwidth* approach. In case of changes for the *large bandwidth* approach, these occur at high data rates, while the *shortest path* has it changes in the lower data rates. Higher data rates such a 54 Mbit/s are achieved rarely.

As seen from Figure 12 and 13 the threshold is an important parameter to investigate. Therefore we present the mean stability time versus a changing threshold in Figure 14. From this figure we can draw the conclusion that the *shortest path* approach is more stable if the threshold value $r_{i\theta}$ is larger than 18 Mbit/s. In case of smaller values for $r_{i\theta}$, the *largest bandwidth* approach is more stable. The reasoning for this behavior was given above.

6. CONCLUSION

We have presented a framework for mobility and stability

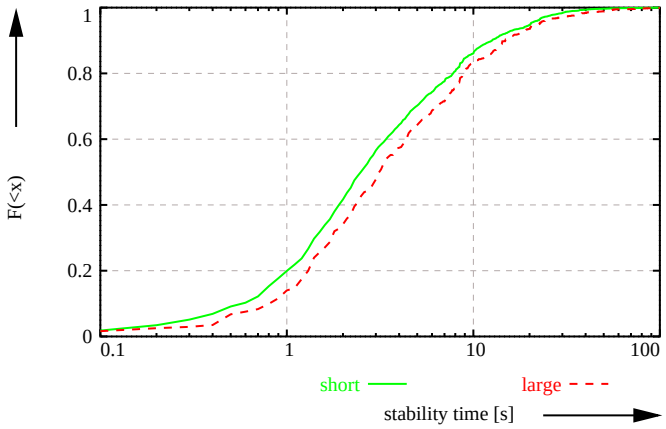

Figure 13: Cumulative stability PDF ψ with threshold of 12 Mbit/s.

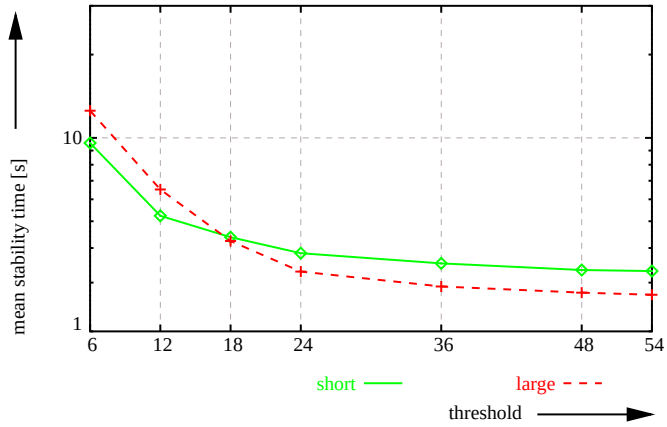

Figure 14: Mean stability time versus threshold $r_{i\theta}$.

measurements for multi-hop networks. This framework can be used with realistic mobility data obtained from measurements obtained by using the multi-player *Quake II* engine. There are many advantages to this approach. First of all, the use of a virtual world for simulation allows to take into account several realistic effects. Obstacles and infrastructure can be considered, not only with respect to preventing connectivity, but also for the mobile users' choice of path. Secondly, the collected data can be used to design new efficient data protocols. Finally, the approach that we have presented is cheap and efficient and can be used for many new applications. Researchers may create their own world, measure the mobility data and investigate the impact on the communication protocol.

In addition, by means of routing protocols for wireless multi-hop networks we have shown the impact of the mobility measurements on the protocol design. Two different routing algorithms were compared, i.e., *shortest path* and *largest bandwidth*, and it was shown that the stability is much higher for the *shortest path* approach if no threshold is given. For smaller threshold values the *largest bandwidth* approach yields better stability values than the *shortest path* approach.

In [15], installation guide for the client software, the used trace files, and an overview of the project including further information is given.

7. OUTLOOK

In our future work we want to investigate more realistic maps. In this work we used only a plain box for our first investigation and to introduce our approach. More advanced maps may contain walls and also make use of the 3rd dimension. In the cases where such maps are used, the radio propagation may also be included into our model. As long as the map is known, the calculation of a direct path should be easy to integrate. To investigate the impact of group mobility we can use team-based games such as *Half-Life*. Unfortunately, the source code for this game is not available at the moment.

Another issue is the impact of the mobility on the communication quality. In the work that we have presented here, the terminals move around without any feedback on their situation. This scenario reflects the situation were multi-hop is applied on terminals that do not know about ongoing transmission; e.g., sensors that are applied to the terminal and sending data to some other terminal (me.g., a terminal with a backbone connection). In such a situation, feedback does not exist. There might, however, be situations were the mobility is directly influenced by the communication quality. This is a known effect, for instance, where mobile phone users with bad reception move towards a window to get a better connection. In the case of cellular communication this might be a negligible issue in terms of the location as the cell is large. But for multi-hop networks this might be an important effect. We will therefore investigate punishing users with bad communication quality by decreasing their view quality within the game or by increasing their ping time. To do so we have to implement our multi-hop calculations into the gaming server software. Thus, the server would have access to the communication quality and give feedback in terms of, e.g., higher ping times. The actual scenario without any feedback allows a decoupling of the measurement on the server and the post-processing of the data.

8. ACKNOWLEDGMENTS

We would like to thank the anonymous students of the University of Ferrara, who were willing to offer their spare time and operate the *Quake II* clients. Furthermore we would like to thank Diego Angelini for his work simulating the link adaptation of IEEE802.11a given in Figure 1.

9. REFERENCES

[1] T. Camp, J. Boleng, and V. Davies. A survey of models for ad hoc network research. *Wireless Communication and Mobile Computing*, 2002.

[2] J. Yoon, M. Liu, and B. Noble. Random waypoint considered harmful. In *Proceedings of INFOCOM 2003*, 2003.

[3] C. Chiang. *Wireless Network Multicasting*. PhD thesis, University of California, Los Angeles, 1999.

[4] E. S. Elmallah, H. S. Hassanein, and H. M. AboElFotoh. On the use of a simple mobility model in ad hoc routing. In *Proc. of International Conference on Parallel Processing Workshops*, pages 479–484, 2001.

[5] J. Tian, J. Hähner, C. Becker, I. Stepanov, and K. Rothermel. Graph-based mobility model for mobile ad hoc network simulation. In *Proc. of 35th Annual Simulation Symposium*, pages 309–316, 2002.

[6] P. Johansson, T. Larsson, N. Hedman, B. Mielczarek, and M. Degermark. Scenario-based performance analysis of routing protocols for mobile ad-hoc networks. In *Proceedings of Mobicom'99*, pages 195–206.

[7] K.H. Wang and B. Li. Group mobility and partition prediction in wireless ad-hoc networks. In *Proceedings of ICC'02*, pages 1017–1021.

[8] IEEE Std 802.11a 1999 . Part 11: Wireless LAN Medium Access Control (MAC) and Physical Layer (PHY) specifications High-speed Physical Layer in the 5 GHz Band. Technical report, IEEE, 1999.

[9] The MathWorks: Developers of Matlab and Simulink. Matlab. `http://www.mathworks.com/` .

[10] B. Bing. *Wireless Local Area Networks*. WILEY, 2002.

[11] F. Fitzek, P. Seeling, M. Reisslein, and M. Zorzi. Visualization Tool for Ad Hoc Networks (ViTAN) – Version 1.0. Technical Report 003-02, acticom, `http://www.acticom.de/vitan.html`, Nov 2002.

[12] BBC News. Quake blows away design problems. `http://news.bbc.co.uk/1/hi/education/982346.stm`, October 2000.

[13] P. Richens. *Playing games*. University of Cambridge, Martin Centre for Architectural and Urban Studies, Cambridge, United Kingdom, 2000. `http://www.arct.cam.ac.uk/research/pubs/pdfs/rich00a.pdf`.

[14] P. Richens. Playing games. *in: Digital Creativity*, 11(3):156–160, 2000.

[15] F. Fitzek. Quake II - Mobility Measurements for Multi Hop Networks . `http://www-tlc.ing.unife.it/new_site/staff/ffitzek/QuakeII.html`, March 2003.

[16] T. Henderson. Observations on game server discovery mechanisms. *Proceedings of the First Workshop on Network and System Support for Games (NetGames2002)*, pages 47–52, April 2002. Braunschweig.

[17] F. Fitzek. Multihop connectivity and bandwidth calculation of arbitrary networks. `http://www-tlc.ing.unife.it/new_site/staff/ffitzek/Manual.pdf`, 2003.

[18] L. E. Miller. Catalog of network connectivity models. `http://w3.antd.nist.gov/wctg/netanal/netanal_netmodels.html`, April 2001.

[19] L. E. Miller. Multihop connectivity of arbitrary networks. `http://w3.antd.nist.gov/wctg/netanal/ConCalc.pdf`, March 2001.

[20] P. Santi and M. D. Blough. The critical transmitting range for connectivity in sparse wireless ad hoc networks. *IEEE Transactions on Mobile Computing*, 2(1):25–39, Jan 2003.

[21] O. Dousse, P. Thiran, and M. Hasler. Connectivity in ad-hoc and hybrid networks. In *Proc. of INFOCOM 2002*, volume 2, pages 1079–1088, 2002.

APPENDIX

```
295309 217.72.69.70:27901 (1056,−10494,5313) − 241ms
295309 217.72.71.96:27901 (−1024,−5120,1282) − 229ms
295309 217.72.90.71:27901 (3136,−7750,3265) − 245ms
295409 217.72.69.70:27901 (1056,−10494,5313) − 240ms
295409 217.72.71.96:27901 (−1024,−5120,1282) − 231ms
295409 217.72.90.71:27901 (3100,−7780,3265) − 249ms
295504 217.72.69.70:27901 (1056,−10494,5313) − 241ms
295504 217.72.71.96:27901 (−1024,−5120,1282) − 226ms
295504 217.72.90.71:27901 (3097,−7781,3265) − 245ms
295600 217.72.69.70:27901 (1056,−10494,5313) − 243ms
295600 217.72.71.96:27901 (−1024,−5120,1282) − 224ms
295600 217.72.90.71:27901 (3097,−7781,3265) − 246ms
```

Listing 1: Example Trace File

$$b_{i,j}^{(m)} = \begin{cases} 0 & : \quad i = j \\ 0 & : \quad c_{i,j}^{(m-1)} > 0 \\ min(c_{i,k}^{(m-1)} + c_{kj}^{(m-1)}) & : \quad \sum_{k-1}^{J} c_{ik}^{(m-1)} \cdot c_{kj}^{(m-1)} > 0 \; when \; i \neq j \; and \; c_{i,j}^{(m-1)} = 0 \\ 0 & : \quad otherwise \end{cases} \tag{13}$$

$$s_{i,j} = \begin{cases} 0 & : \quad single \; hop \; i \leftrightarrow j \; does \; not \; exist \rightarrow d_{i,j} > D_{MAX} \\ 6 & : \quad single \; hop \; i \leftrightarrow j \; exists \rightarrow D_{12} \leq d_{i,j} < D_6 \\ 12 & : \quad single \; hop \; i \leftrightarrow j \; exists \rightarrow D_{18} \leq d_{i,j} < D_{12} \\ 18 & : \quad single \; hop \; i \leftrightarrow j \; exists \rightarrow D_{24} \leq d_{i,j} < D_{18} \\ 24 & : \quad single \; hop \; i \leftrightarrow j \; exists \rightarrow D_{36} \leq d_{i,j} < D_{24} \\ 36 & : \quad single \; hop \; i \leftrightarrow j \; exists \rightarrow D_{48} \leq d_{i,j} < D_{36} \\ 48 & : \quad single \; hop \; i \leftrightarrow j \; exists \rightarrow D_{54} \leq d_{i,j} < D_{48} \\ 54 & : \quad single \; hop \; i \leftrightarrow j \; exists \rightarrow d_{i,j} < D_{54} \end{cases} \tag{14}$$

$$\rho'_{s,i} = \frac{\text{number of}(\{t \; : \; r_i[t] \neq r_i[t-1]\}) + (k-1)\text{number of}(\{t \; : \; (r_i[t] > r_{\theta,i}\text{XOR}r_i[t-1] > r_i\theta) == 1\})}{\text{total number of samples}}. \tag{15}$$